

## Search for the $l$ -forbidden beta decay $^{207}\text{Tl} \rightarrow ^{207}\text{Pb}^*(570 \text{ keV})$

M. M. Hindi\*

*University of Petroleum and Minerals, Dhahran, Saudi Arabia*

E. G. Adelberger, S. E. Kellogg,<sup>†</sup> and T. Murakami<sup>‡</sup>

*Nuclear Physics Laboratory GL-10, University of Washington, Seattle, Washington 98195*

(Received 16 May 1988)

We have searched for the  $l$ -forbidden beta decay of  $^{207}\text{Tl}$  to the first excited state of  $^{207}\text{Pb}$  by looking for 570-keV  $\gamma$  rays following the decay of  $^{207}\text{Tl}$ . We find a branching ratio of  $(2.4 \pm 5.6) \times 10^{-7}$  per  $^{207}\text{Tl}$  decay. This limit could provide a test for calculations of core polarization, meson exchange, and  $\Delta$  excitation effects. We also find a branch of  $(0.54 \pm 0.05)\%$  for the  $l$ -forbidden  $M1$  transition  $^{207}\text{Pb}(898, \frac{3}{2}^- \rightarrow 570, \frac{3}{2}^-)$  and measure the intensities of  $\gamma$  rays emitted following the decay of  $^{211}\text{Pb}$ .

### I. INTRODUCTION

The  $\frac{1}{2}^+ \rightarrow \frac{3}{2}^-$   $\beta$  decay of  $^{207}\text{Tl}$  to the 570-keV first excited state of  $^{207}\text{Pb}$  is a unique first-forbidden decay. The  $^{207}\text{Tl}$  ground state is, to first order, a  $3s_{1/2}$  proton hole and the  $^{207}\text{Pb}$  570-keV state is a  $2f_{5/2}$  neutron hole. Thus the orbital angular momentum change involved in the decay is  $\Delta l = 3$ . The first-forbidden decay operator, however, changes the orbital angular momentum by one unit; therefore, to first order this decay is  $l$  forbidden as well.<sup>1</sup> The decay rate is thus expected to be dominated by corrections to the wave functions and to the decay operator due to core polarization,  $\Delta - N^{-1}$  admixtures, and exchange currents.<sup>2</sup> With the aim of providing an observable which can shed light on these "extra-nucleonic" degrees of freedom, we have attempted to measure the aforementioned decay rate by looking for 570-keV  $\gamma$  rays following the decay of  $^{207}\text{Tl}$ .

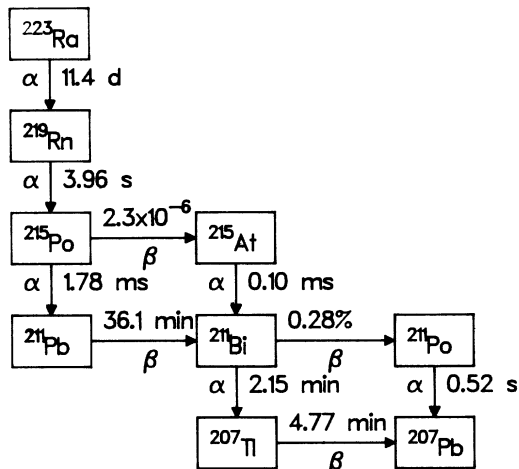
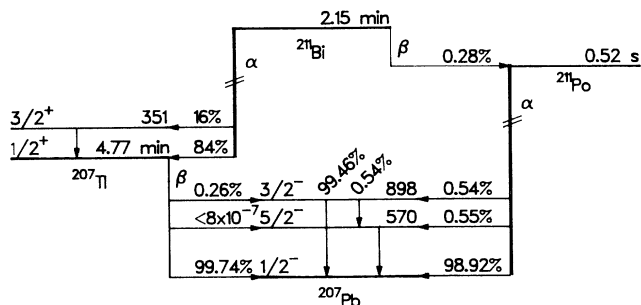
While the contribution of such "extra-nucleonic" degrees of freedom to magnetic moments and  $l$ -forbidden  $M1$  transitions in the  $^{208}\text{Pb}$  region has been studied extensively both theoretically and experimentally,<sup>2,3</sup> the study of their contribution to  $l$ -forbidden beta decays has been sparse. A notable exception is the recent work of Adelberger *et al.*,<sup>4</sup> who measured the  $l$ -forbidden beta decay rate of  $^{39}\text{Ca}(\frac{1}{2}^+)$  to  $^{39}\text{K}^*(\frac{1}{2}^+)$ . Both  $^{207}\text{Tl}$  and  $^{39}\text{Ca}$  are one nucleon removed from a doubly-magic nucleus, and hence the zero-order wave functions can be determined reliably. However,  $^{39}\text{Ca}$  is a hole in an  $LS$  closed shell and hence the contribution of core polarization enters only in second order, compared to meson exchange and isobar currents which contribute in first order.<sup>4</sup> In  $^{207}\text{Tl}$  the shells are  $jj$  closed and hence core polarization contributes in first order. Consequently, one would expect that the weights of various contributions to the  $l$ -forbidden decay of  $^{207}\text{Tl}$  will be different from those in the  $l$ -forbidden decay of  $^{39}\text{Ca}$  and hence that the current experiment would provide an independent measurement of the various couplings.

In the course of our experiment we also measured the intensity of  $\gamma$  rays following the beta decay of  $^{211}\text{Pb}$ .

Since the precision of our measurement is comparable to the most precise data available in the literature, we felt it worthwhile to present these data as well.

### II. EXPERIMENTAL PROCEDURE

The  $^{207}\text{Tl}$  activity was produced from the decay chain of  $^{223}\text{Ra}$  (Fig. 1). A  $1.9 \times 10^7$  Bq (0.5 mCi) source of  $^{223}\text{Ra}$  in a 0.5 N HCl solution was obtained from Isotope Products Laboratories, Burbank, California. The solution was deposited onto a cation exchange column (Dowex 50 W X4, 100–200 mesh, Hydrogen form)  $\approx 3$  cm high and 0.8 cm in diameter. The  $^{207}\text{Tl}$  activity was eluted from the column with 0.5 N HCl. The above procedure is similar to that of Ref. 5. The solution was eluted into a 4 ml vial which was taken to a counting station (described below), and counted for 800 s ( $\approx 2.8$  times the  $^{207}\text{Tl}$  half-life of 4.77 min). This simple radiochemical procedure did not completely separate the Tl and Bi activities. In particular, the presence of  $^{211}\text{Bi}$  ( $t_{1/2} = 2.15$  min) proved troublesome because (1) the intense 351-keV  $^{211}\text{Bi}$  line dominated the count rate, and (2) the 570-keV gamma line of interest is produced via weak branchings through  $^{211}\text{Po}$  (Fig. 2.). In order to reduce these problems, the sample was not counted until approximately 6 min after elution or until the count rate in the Ge(Li) detector dropped to  $\approx 6$  kHz. Since the elution process had to be repeated several times in order to accumulate enough statistics, Pb, whose distribution coefficient is  $\approx 4$  (compared to  $\approx 0.4$  for Tl and  $\approx 100$  for Ra),<sup>6</sup> was eventually also eluted from the solution. The vial with the eluted solution was placed in a plexiglas sleeve attached to the front face of a 45 cm<sup>3</sup> Ge(Li) detector. The walls of the plexiglas sleeve were  $\approx 6$  mm thick in order to stop betas accompanying the decay of  $^{207}\text{Tl}$ . The Ge(Li) detector was surrounded by a NaI shield consisting of an annular detector 30.0 cm long  $\times$  21.5 cm outer diameter with an 8.9 cm inner diameter, and a 7.6 cm  $\times$  7.6 cm NaI detector to close one end of the annulus. The NaI array had two functions: (1) it acted as an anticoincidence shield and (2) it suppressed 570-keV transitions fed by the  $\gamma$  decay of the 898-keV level by

FIG. 1. Decay chain of  $^{223}\text{Ra}$ .FIG. 2. Decay schemes of  $^{211}\text{Bi}$ ,  $^{211}\text{Po}$ , and  $^{207}\text{Tl}$ . Level energies are in keV.

detecting the accompanying 328-keV  $\gamma$  ray in anticoincidence (Fig. 2). A standard fast-slow coincidence circuit routed the Ge(Li) signal into one of two 2048-channel regions in an ND2400 multichannel analyzer: one region for no-coincidence signals (labeled ACCEPTS) and one for coincidence signals (labeled REJECTS). The

TABLE I. Gamma rays observed in the elution of  $^{207}\text{Tl}$  from  $^{223}\text{Ra}$ .<sup>a</sup>

Parent nuclide	$E_\gamma$ (keV)		$I_\gamma$ (relative)	
	Present work	Ref. 7	Present work	Ref. 7
$^{211}\text{Bi}$	351.06(12)	351.00(10)		
$^{207}\text{Tl}$	328.10(12)	328.2(2)		
$^{207}\text{Tl}$	569.62(12)	569.65(10)	(see Table IV)	
$^{207}\text{Tl}$	897.77(12)	897.80(10)		
$^{214}\text{Bi}$	609.32(12)	609.312(10)	46.1(1.5) <sup>b</sup>	46.1(1.2)
$^{214}\text{Bi}$	665.27(14)	665.453(22)	1.64(31)	1.59(5)
$^{214}\text{Bi}$	768.45(12)	768.356(10)	4.56(29)	5.00(7)
$^{214}\text{Bi}$	805.98(12)	806.174(18)	1.18(12)	1.25(3)
$^{214}\text{Bi}$	826.31(24)	826.2(3)	0.32(10)	0.090(7)
$^{214}\text{Bi}$	934.05(12)	934.061(14)	3.26(19)	3.25(6)
$^{214}\text{Bi}$	1120.26(12)	1120.287(2)	15.1(6)	15.3(2)
$^{214}\text{Bi}$	1155.21(16)	1155.19(2)	1.87(16)	1.72(5)
$^{214}\text{Bi}$	1238.13(15)	1238.110(10)	5.62(28)	6.05(6)
$^{214}\text{Bi}$	1281.03(22)	1280.96(2)	1.46(16)	1.50(5)
$^{214}\text{Bi}$	1377.64(19)	1377.669(14)	3.66(21)	4.12(8)
$^{214}\text{Bi}$	1385.30(26)	1385.31(3)	0.81(12)	0.79(3)
$^{214}\text{Bi}$	1401.60(26)	1401.50(4)	1.32(16)	1.41(4)
$^{214}\text{Bi}$	1407.94(25)	1407.98(4)	2.13(18)	2.52(4)
$^{214}\text{Bi}$	1509.21(27)	1509.228(17)	2.17(20)	2.23(5)
$^{214}\text{Pb}$	242.01(12)	241.92(3)	8.3(4)	7.6(8)
$^{214}\text{Pb}$	295.17(12)	295.22(4)	18.9(6) <sup>b</sup>	18.9(2)
$^{227}\text{Th}$	235.92(14)	236.0(2)	100(9) <sup>b</sup>	100(8)
$^{227}\text{Th}(?)$	254.2(3)	254.7	25(9)	3.8(8)
$^{227}\text{Th}$	256.16(16)	256.3(2)	56(8)	57(3)
$^{227}\text{Th}$	285.5(5)	286.2(2)	16(9)	12.3(6)
$^{227}\text{Th}$	298.2(6)	300.0(2)	16(9)	17(2)
$^{227}\text{Th}$	329.9(2)	329.9(2)	44(10)	21.5(1.5)

<sup>a</sup>  $^{211}\text{Pb}$  lines are listed in Table II.<sup>b</sup> Yield normalized to that in Ref. 7. See Table III for yield relative to  $^{207}\text{Tl}(898)$  line.

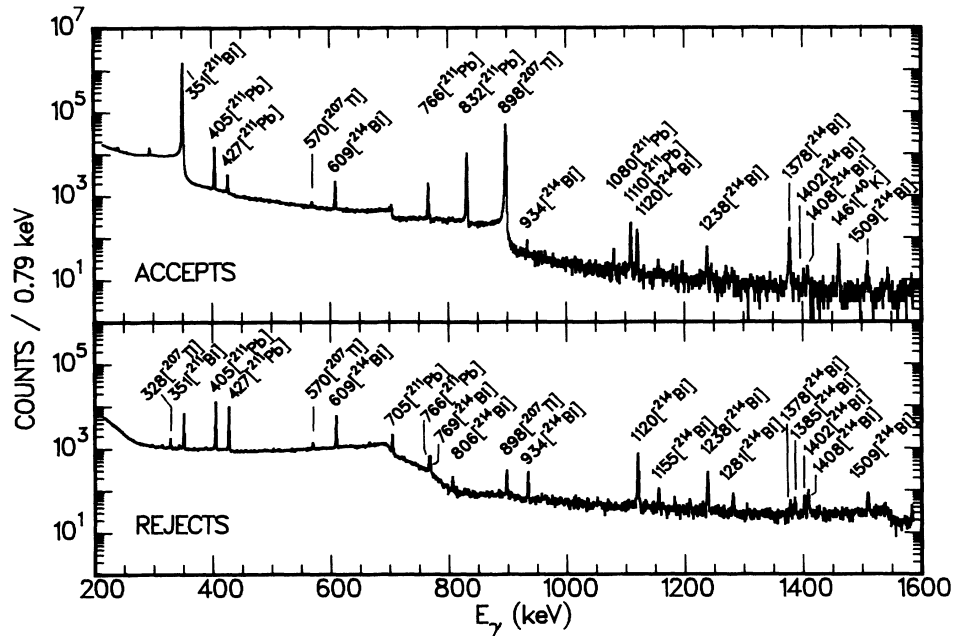


FIG. 3. Gamma-ray spectrum observed after the elution of  $^{207}\text{Tl}$  from  $^{227}\text{Ra}$ . The lower spectrum (REJECTS) corresponds to counts vetoed by the anticoincidence shield, the upper spectrum (ACCEPTS) corresponds to counts without coincidence. Gamma rays are labeled by their energy, to the nearest keV, and by their parent nuclide.

accidental coincidence rate was kept below 1% (typically 0.5%) without having to reject slow risetime signals. In a preliminary set of runs the spectra were collected using a PDP 11/60 data acquisition system. For those runs, the ACCEPTS and REJECTS spectra were collected in four successive time slices each 4 min long.

The energy calibration and the efficiency of the Ge(Li) detector as a function of energy were determined using calibrated sources of  $^{54}\text{Mn}$ ,  $^{57}\text{Co}$ ,  $^{60}\text{Co}$ ,  $^{88}\text{Y}$ ,  $^{133}\text{Ba}$ ,  $^{137}\text{Cs}$ , and  $^{207}\text{Bi}$ .

### III. EXPERIMENTAL RESULTS

A cumulative spectrum representing 4.44 h of counting is shown in Fig. 3. An expanded view of the region of the

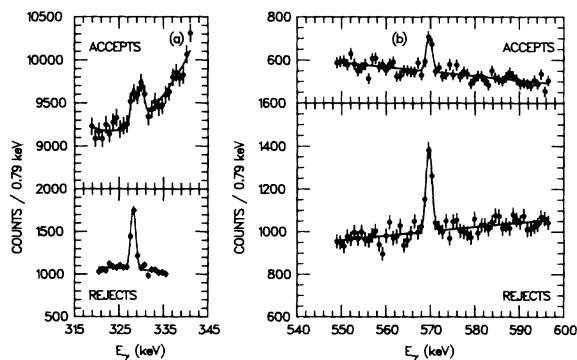


FIG. 4. Expanded regions from Fig. 3: (a) region of the 328-keV peak, (b) region of the 570-keV peak. The lines are fits with Gaussian shapes plus polynomial background.

328- and 570-keV lines is shown in Fig. 4. The strongest lines shown in Fig. 3 are labeled by their approximate energy and parent nuclide. In addition to the 328-, 570-, and 898-keV  $\gamma$  rays from  $^{207}\text{Tl}$  decay, we observed  $\gamma$  rays from the  $^{211}\text{Bi}$  and  $^{211}\text{Pb}$  parents of  $^{207}\text{Tl}$ , and from  $^{214}\text{Pb}$ ,  $^{214}\text{Bi}$  ( $^{226}\text{Ra}$  daughters) and  $^{227}\text{Th}$  contaminants in the  $^{223}\text{Ra}$  source. The decay half-lives of the 351- and 898-keV lines were obtained from the set of time-gated spectra mentioned above and were found to be consistent with those of  $^{211}\text{Bi}$  and  $^{207}\text{Tl}$ , respectively.

The intensities of the 351- and 898-keV lines in the REJECTS spectrum shown in Fig. 3 are  $(0.392 \pm 0.006)\%$  and  $(0.47 \pm 0.04)\%$ , respectively, of their intensities in the ACCEPTS spectrum. These fractions are consistent with the expected accidentals rate. The slightly higher fraction of rejected 898-keV gammas may be due to real coincidences between the 898-keV  $\gamma$  ray and bremsstrahlung from the beta ray feeding the 898-keV level. Thus we conclude that no  $\gamma$  rays accompany the 351- and 898-keV  $\gamma$  rays, which is consistent with the decay schemes of  $^{211}\text{Bi}$  and  $^{207}\text{Tl}$  (Fig. 2 and Ref. 7). Because of this, and the agreement of the energy of these lines,  $351.06 \pm 0.12$  keV and  $897.77 \pm 0.12$  keV, with the energies<sup>8</sup>  $351.0 \pm 0.1$  keV and<sup>9</sup>  $897.8 \pm 0.1$  keV of the  $\gamma$  rays from the decay of  $^{211}\text{Bi}$  and  $^{207}\text{Tl}$ , respectively, we ascribe the 351-keV line to  $^{211}\text{Bi}$  decay and the 898-keV line predominantly to  $^{207}\text{Tl}$  decay.

Table I lists the  $\gamma$  rays observed in the spectrum shown in Fig. 3. The  $^{211}\text{Pb}$  lines, shown in Table II, were extracted from separate spectra collected as follows: a volume saturated with Pb was eluted and counted for two time periods each 2000 s and separated by 49 min. The total spectrum is shown in Fig. 5. These spectra were used to obtain (1) much better statistics on the  $^{211}\text{Pb}$  lines,

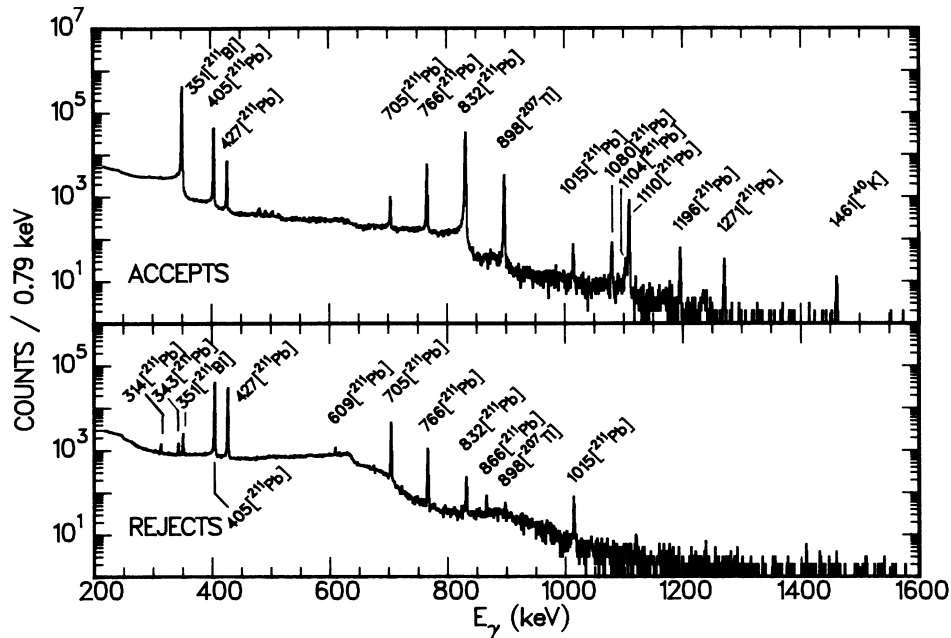


FIG. 5. Spectra of gamma rays vetoed by the anticoincidence shield (REJECTS) and not vetoed (ACCEPTS), following the elution of  $^{211}\text{Pb}$  from  $^{223}\text{Ra}$ .

TABLE II.  $^{211}\text{Pb}$  gamma rays observed in elution of Pb from  $^{223}\text{Ra}$ .

$E_\gamma$ (keV)	Relative intensity <sup>a</sup>						Present work	
	Present work	Ref. 10	Ref. 10	Ref. 11	Ref. 12	Ref. 8		Average <sup>b</sup>
313.64(12)		313.8(2)	0.24(3)					
342.02(12)		342.7(2)	0.27(4)	0.15(5)	0.22(3)	0.25(2)		
404.89(12)		404.84(4)	30.0(9)	27.4(1.2)	29.6(2.0)	30.8(1.5)	29.6(6)	29.3(9)
427.14(12)		426.99(4)	13.5(6)	14.5(1.4)	13.7(1.0)	14.3(8)	13.8(4)	13.9(4)
		478.0(4)	0.10(2)					
479.62(20)								0.04(1)
		481.1(4)	0.20(4)					
481.92(12)								0.08(1)
491.82(12)		492.0(4)	0.11(3)					0.032(6)
494.22(30)								0.013(5)
		500.4(5)	0.09(2)					
502.02(20)								0.028(6)
504.12(12)		503.3(4)	0.12(2)					0.045(6)
		503.6(7)			0.006			
		609.5(2)	0.18(3)		0.25(5)	<0.41	0.20(3)	
704.66(12)		704.5(1)	3.77(19)		3.7(3)	3.7(2)	3.73(13)	3.6(1)
766.45(12)		766.34(7)	5.55(28)	5.2(2)	4.9(3)	5.0(3)	5.18(13)	4.94(16)
832.02(12)		831.83(4)	29.8(9)	27.4(1.2)	24.1(1.7)	25.6(2.3)	28.05(6)	26.7(8)
865.87(24)		865.6(3)	0.050(8)		0.07(2)	0.053(15)	0.053(7)	0.042(6)
1014.71(12)		1014.7(2)	0.14(1)		0.15(1)	0.13(2)	0.144(7)	0.129(8)
1080.10(13)		1080.2(1)	0.120(12)		0.08(1)	0.083(10)	0.091(6)	0.095(6)
1103.52(20)		1103.4(4)	0.040(6)			0.023(5)	0.030(4)	0.033(4)
1109.48(13)		1109.5(2)	1.15(8)		0.81(6)	0.79(8)	0.895(41)	0.90(3)
1196.15(14)		1196.6(2)	0.10(1)		0.08(1)	0.079(15)	0.088(6)	0.072(5)
1270.79(18)		1270.8(2)	0.070(7)		0.08(1)	0.048(8)	0.065(5)	0.043(4)

<sup>a</sup>Intensities relative to  $I_\gamma = 100$  for the 351-keV  $\gamma$  ray of  $^{211}\text{Bi}$ , with  $^{211}\text{Bi}$   $\alpha$  decay in equilibrium.

<sup>b</sup>Weighted average of intensities given in columns 3–6.

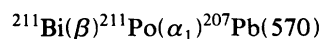
(2) a two point half-life estimate of the lines attributed to  $^{211}\text{Pb}$ , and (3) the branching ratio of  $^{207}\text{Tl}$  to the 898-keV level in  $^{207}\text{Pb}$ , as explained below. The assignment of  $\gamma$  rays shown in Tables I and II to the indicated parent nuclides rests on the agreement of their energies and relative intensities with the accepted values for these quantities.<sup>7</sup> As Table II shows, our results for the relative intensities of  $^{211}\text{Pb}$  transitions agree well with the weighted average of the previously reported results.<sup>8,10-12</sup> Although we do observe  $\gamma$  rays in the region 65-97 keV, our resolution at those energies was not good enough to separate those from Pb x rays and from each other. We do observe six weak lines between 479 and 505 keV but these are not in agreement with the lines given in that energy region in Ref. 10. Because these lines are not accompanied by any transitions (all the strength is in the ACCEPTS spectrum), it is unlikely that these transitions are in  $^{211}\text{Pb}$ . However, the overall agreement of the extracted relative intensities for lines we do associate with the decay of  $^{211}\text{Pb}$  with previously published results assures us that our energy and efficiency calibrations are correct.

Because the contaminants observed in our spectra have complicated decay schemes, it is important to ascertain that the 570- and 328-keV lines, which are the weak lines of interest in this study, actually belong to transitions in  $^{207}\text{Pb}$  resulting from  $^{207}\text{Tl}$  (and  $^{211}\text{Po}$ ) decay, and are not some weak previously unreported transitions in the contaminants that are accidentally degenerate with the sought-after lines. To that end we compared the contaminants yield in the PDP-11 run to their yield in the ND2400 run. Because of variations in the eluant volume, delay time between elution and counting and possibly some other factors, the yield of contaminants relative to the yield of the 898-keV  $^{207}\text{Tl}$   $\gamma$  rays is different in the two runs. If we let  $R1(E)$ =(yield of  $\gamma$ 's of energy  $E$ )/(yield of 898-keV  $\gamma$ 's) for the ND2400 spectrum (Fig. 3), and  $R2(E)$  the corresponding ratio for the PDP-11 spectrum, then  $R=R1/R2$  is a measure of the correlation between  $\gamma$  rays of energy  $E$  with that of the 898-keV line. Table III shows these ratios for the strongest transitions identified with each of the contaminants as well as

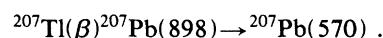
for the 570- and 328-keV lines. It is clear from the table that the relative yield of contaminants changed substantially while that of the 570- and 328-keV lines remained correlated with the yield of the 898-keV transition in  $^{207}\text{Pb}$ . Hence we are confident that these transitions are in  $^{207}\text{Pb}$ . Since the  $\beta^+ / EC$  decay of  $^{207}\text{Bi}$  can also feed the states of interest, we searched for the 1063.64-keV  $\gamma$  ray line that would be present in  $^{207}\text{Bi}$  decay (but not in  $^{207}\text{Tl}$  or  $^{211}\text{Po}$  decay).<sup>7</sup> (Although  $^{207}\text{Bi}$  is an unlikely contaminant in the  $^{223}\text{Ra}$  solution, it is a possible contaminant in the Pb shielding surrounding the annular NaI detector.) No evidence for this line was found; its yield relative to that of the 570-keV line was  $< 2.5 \times 10^{-2}$  (one standard deviation), compared to  $0.755 \pm 0.023$  expected for  $^{207}\text{Bi}$  decay.<sup>9</sup>

The  $\gamma$  ray yield of the 570- and 328-keV lines was extracted using a Gaussian peak shape plus a polynomial background. These fits are shown in Fig. 4. The peak on the high-energy side of the 328-keV  $^{207}\text{Tl}$  line [Fig. 4(a)] has an energy of  $329.9 \pm 0.2$  keV and is probably mostly due to  $^{227}\text{Th}$  (see Table I).

In extracting the beta branch of  $^{207}\text{Tl}$  to the 570-keV level corrections have to be made for the indirect feedings



and



Because the observed yield of 570-keV  $\gamma$  rays is consistent with that from the above indirect feedings, the extracted branch is very sensitive to these corrections. Therefore, we believe it is important to detail how these corrections were made. The observed total photopeak area (ACCEPTS plus REJECTS) of 570-keV  $\gamma$  rays,  $YTOT_{570}$ , is related to the number of feedings from  $^{207}\text{Tl}$ ,  $N_{\text{Tl}}$ , and from  $^{211}\text{Po}$ ,  $N_{\text{Po}}$ , and from the decays  $^{207}\text{Pb}(898) \rightarrow ^{207}\text{Pb}(570)$ ,  $N_{328}$ , by

$$YTOT_{570} = \epsilon_{570}(1 + \alpha_{570})^{-1} [N_{\text{Tl}} + N_{\text{Po}} + N_{328}(1 - P_{\text{sum}})] ,$$

where

$$P_{\text{sum}} = (1 + \alpha_{328})^{-1} \eta_{328} + \alpha_{K,328}(1 + \alpha_{328})^{-1} \omega_K \eta_K ,$$

TABLE III. Intensity of gamma ray lines relative to 898-keV line.<sup>a</sup>

Parent nuclide	$E_\gamma$ (keV)	ND2400 run (%)	PDP-11 run (%)	Ratio (ND2400/PDP-11)
$^{207}\text{Tl}$	570	0.57(4)	0.59(6)	0.97(12)
$^{207}\text{Tl}$	328	0.50(5)	0.61(6)	0.82(12)
$^{211}\text{Bi}$	351	831(7)	954(7)	0.87(1)
$^{211}\text{Pb}$	405	19.0(1)	105.5(8)	0.180(2)
$^{211}\text{Pb}$	832	17.5(1)	96.6(5)	0.181(1)
$^{214}\text{Pb}$	242	0.82(4)	0.26(9)	3(1)
$^{214}\text{Pb}$	295	1.86(5)	0.6(1)	3.1(6)
$^{214}\text{Bi}$	609	7.40(7)	1.18(13)	6.3(7)
$^{214}\text{Bi}$	1120	2.38(6)	0.37(2)	6.5(5)
$^{227}\text{Th}$	236	0.44(4)	2.99(9)	0.15(2)
$^{227}\text{Th}$	256	0.25(4)	1.77(12)	0.14(2)

<sup>a</sup>Only strongest two lines of each nuclide is given. Intensities of other lines can be determined from the relative intensities given in Table I.

and  $\epsilon_{570}$  is the Ge(Li) photopeak efficiency for 570-keV  $\gamma$  rays,  $\alpha$  is the total internal conversion coefficient,  $\alpha_K$  is the  $K$ -shell internal conversion coefficient,  $\eta_{328}$  is the Ge(Li) total efficiency for 328-keV  $\gamma$  rays,  $\omega_K$  is the  $K$ -shell fluorescence yield, and  $\eta_K$  is the Ge(Li) total efficiency for Pb  $K$  x rays.  $P_{\text{sum}}$  is the probability that a 570-keV  $\gamma$  ray that is fed by a transition from  $^{207}\text{Pb}(898)$  to  $^{207}\text{Pb}(570)$  is summed out of the photopeak by the accompanying radiation from that transition. That radiation could be a 328-keV  $\gamma$  ray or an x ray following a transition by internal conversion. Internal conversion from shells higher than the  $K$  shell has been ignored in the above expression because both the  $M1$  internal conversion coefficients for those shells and the Ge(Li) efficiency for the low-energy radiation filling the holes are small. Internal conversion electrons are absorbed by the source holder and hence do not contribute to summing. The photopeak area of 570-keV  $\gamma$  rays in the ACCEPTS spectrum,  $YACC_{570}$ , is related to the feedings of the 570-keV level by

$$YACC_{570} = \epsilon_{570}(1 + \alpha_{570})^{-1} \\ \times [N_{\text{Tl}} + N_{\text{Po}} + N_{328}(1 - P_{\text{sum}} - P_{\text{shield}})],$$

where

$$P_{\text{shield}} = (1 + \alpha_{328})^{-1}(\xi_{328} - \zeta_{328}) \\ + \alpha_{K,328}(1 + \alpha_{328})^{-1}\omega_K(\xi_K - \zeta_K),$$

$\xi$  is the anticoincidence shield efficiency, and  $\zeta$  is the fraction of  $\gamma$  rays (or x rays) that enters the shield by scattering from the Ge(Li) detector.  $P_{\text{shield}}$  is the probability that radiation accompanying the feeding of the 570-keV level by a transition from  $^{207}\text{Pb}(898)$  to  $^{207}\text{Pb}(570)$  is detected by the shield (hence putting the 570-keV signal in the REJECTS route). The fraction of events in which radiation scatters from the Ge(Li) to the shield has to be subtracted from the efficiency of the shield because those events lead to summing in the Ge(Li) and hence are already accounted for in the term  $P_{\text{sum}}$ .

The fraction of events that scatter from the Ge(Li) to the shield was obtained from the ratio of Compton events in the REJECTS spectrum to the calculated yield of absolutely calibrated single-line sources. The anticoincidence shield efficiency was determined from expressions similar to the ones given above applied to coincident transitions in the decays of  $^{60}\text{Co}$ ,  $^{214}\text{Bi}$ ,  $^{207}\text{Bi}$ ,  $^{211}\text{Pb}$ , and  $^{133}\text{Ba}$ .<sup>13</sup>  $N_{\text{Po}}$  was determined from the number of 351-keV  $^{211}\text{Bi}$   $\gamma$  rays observed in our spectrum using the following fractions:  $0.127 \pm 0.002$  351-keV  $\gamma$  rays per  $^{211}\text{Bi}$  decay,<sup>8</sup>  $(2.74 \pm 0.04) \times 10^{-3}$   $\beta^-$  decays to  $^{211}\text{Po}$  per  $^{211}\text{Bi}$  decay,<sup>5</sup> and  $(5.34 \pm 0.19) \times 10^{-3}$  570-keV  $\gamma$  rays per  $^{211}\text{Po}$  decay.<sup>8</sup> The fraction of 570-keV  $\gamma$  rays attributable to  $^{211}\text{Po}$  decay thus extracted was  $(56 \pm 2)\%$  of the ACCEPTS counts and  $(16.5 \pm 0.7)\%$  of the TOTAL=ACCEPTS+REJECTS counts. The errors quoted on these percentages reflect the combined uncertainties in the above branching ratios and the statistical uncertainty in the 351-keV  $\gamma$  ray yield; it does *not* include the statistical uncertainty in the 570-keV  $\gamma$  ray yield.

In order to determine  $N_{328}$  from the observed yield of

328-keV  $\gamma$  rays, the internal conversion coefficient  $\alpha_{328}$  has to be known. There is no previous experimental determination of this coefficient. A theoretical estimate of  $\alpha_{328} = 0.353$  can be obtained from the tables of Rosel *et al.*;<sup>14</sup> however, because the  $898 \rightarrow 570$  transition is to first order a  $3p_{3/2} \rightarrow 2f_{5/2}$   $\Delta l = 2$   $M1$  transition, it is  $l$  forbidden and hence the nuclear structure-dependent penetration effect correction to the above calculation might be very important.<sup>15</sup> By comparing the REJECTS yields of the 570- and 328-keV  $\gamma$  rays we find  $\alpha_{328} = 0.16 \pm 0.08$ . Even though this estimate has a large error it does seem to indicate that the internal conversion coefficient for this transition is less than the first-order theoretical estimate quoted above.

With the above corrections, and making use of the known<sup>9</sup> internal conversion coefficients of the 570- and 898-keV transitions  $(2.20 \pm 0.07)\%$  and  $(2.25 \pm 0.30)\%$ , respectively, we obtain a relative branching ratio

$${}^{207}\text{Tl}(\beta^-) {}^{207}\text{Pb}(570) / {}^{207}\text{Tl}(\beta^-) {}^{207}\text{Pb}(898) \\ = (0.9 \pm 2.1) \times 10^{-4}.$$

To convert this branching ratio to an absolute decay rate the decay rate to the 898-keV state is needed. We obtained the branching ratio of  $^{207}\text{Tl}$  to the 898-keV level from the two spectra whose sum is shown in Fig. 5. From the intensities of the  $^{211}\text{Pb}$  lines, the 351-keV  $^{211}\text{Bi}$  line and the 898-keV  $^{207}\text{Tl}$  lines in each of the two spectra, and making use of the known half-lives of  $^{211}\text{Pb}$  ( $36.1 \pm 0.2$  min),  $^{211}\text{Bi}$  (2.15 min), and  $^{207}\text{Tl}$  ( $4.77 \pm 0.01$  min),<sup>7</sup> and of the intensity of 351-keV  $\gamma$  rays per  $^{211}\text{Bi}$  decay ( $0.127 \pm 0.002$ ),<sup>8</sup> we obtain a value of  $(0.263 \pm 0.009)\%$  for the intensity of 898-keV  $\gamma$  rays per  $^{207}\text{Tl}$  decay. This result is in agreement with, but has a smaller error than the intensities listed in Lederer and Shirley:<sup>7</sup>  $(0.24 \pm 0.04)\%$  (Ref. 5) and  $(0.270 \pm 0.025)\%$ .<sup>8</sup> Combining this result with the branching ratio quoted above we obtain a branching ratio for the beta decay of  $^{207}\text{Tl}$  to the 570-keV level of  $^{207}\text{Pb}$  of  $(2.4 \pm 5.6) \times 10^{-7}$ . This limit is more than 2 orders of magnitude lower than the previously established limit<sup>8</sup> of  $< 1 \times 10^{-4}$ . We also obtain a more precise result for the relative  $\gamma$  ray intensity of the 328-keV line to the 898-keV line:  $(0.54 \pm 0.05)\%$  compared to the previous value<sup>9</sup> of  $(0.6 \pm 0.2)\%$ . Our results are summarized in Table IV.

TABLE IV. Summary of present results.

Beta decay of $^{207}\text{Tl}$	Intensity per decay	
	Present results	Previous results
$^{207}\text{Tl} \rightarrow ^{207}\text{Pb}(898)$	$(2.63 \pm 0.09) \times 10^{-3}$	$(2.40 \pm 0.40) \times 10^{-3}$ <sup>a</sup> $(2.70 \pm 0.25) \times 10^{-3}$ <sup>b</sup>
$^{207}\text{Tl} \rightarrow ^{207}\text{Pb}(570)$	$(2.4 \pm 5.6) \times 10^{-7}$	$< 10^{-4}$ <sup>a</sup>
Radiative decay of $^{207}\text{Pb}(898)$ state	Present result	Previous result
$898 \rightarrow 570 / 898 \rightarrow \text{g.s.}$	$(0.54 \pm 0.05)\%$	$(0.6 \pm 0.2)\%$ <sup>c</sup>

<sup>a</sup>Reference 5.

<sup>b</sup>Reference 8.

<sup>c</sup>Reference 9.

## IV. DISCUSSION AND CONCLUSION

Our measured branch for the  $l$ -forbidden unique beta transition  $^{207}\text{Tl}(\frac{1}{2}^+) \rightarrow ^{207}\text{Pb}(\frac{5}{2}^-)$  corresponds to a half-life  $t_{1/2} > 3.6 \times 10^8$  s (one standard deviation). The only theoretical estimate, to our knowledge, is a calculation by Khafizov using the methods of finite Fermi systems theory (FFST).<sup>16</sup> Taking account of the spin-isospin interaction with the constant  $g'_0 = 1.0$  and of one pion exchange,<sup>16,17</sup> Khafizov gets  $t_{1/2} = 2.3 \times 10^9$  s. If the term  $\lambda[(\sigma \cdot \mathbf{p})\mathbf{p}/p_F^2]\tau_{\pm}$ , is included in the local charge of the quasiparticles, with  $\lambda = 0.03$ , Khafizov gets  $t_{1/2} = 5.5 \times 10^8$  s.<sup>18</sup> A further reduction to  $t_{1/2} \approx 1 \times 10^7$  s is obtained if the velocity-dependent spin-isospin interaction of the quasiparticles,  $g'_1(\sigma_1 \cdot \sigma_2)(\mathbf{p}_1 \cdot \mathbf{p}_2)(\tau_1 \cdot \tau_2)/p_F^2$ , is included with  $g'_1 \approx 0.8$ . It is seen that our result already places a constraint on the  $g'_1$ - $\lambda$  parameter space. The above value of  $\lambda$  was adjusted by Khafizov<sup>18</sup> to fit the measured half-life of the  $l$ -forbidden  $\frac{3}{2}^+ \rightarrow \frac{1}{2}^+$  transition of  $^{39}\text{Ca}$ .<sup>4</sup> The possible influence of a velocity-dependent spin-isospin interaction on that half-life was not explored in Ref. 18 and hence we cannot say whether the value of  $\lambda$  is consistent with our measurement. All we can say is that if  $g'_1 \approx 0$  then the value of  $\lambda$  extracted from the fit to the  $^{39}\text{Ca}$  half-life predicts a half-life that is consistent with our measurement. Plans are currently under way to improve our measurement.

From our measured branching ratio for the  $^{207}\text{Pb}(898, \frac{3}{2}^- \rightarrow 570, \frac{5}{2}^-)$   $\gamma$  transition and the known

half-life of the 898-keV state  $[(0.111 \pm 0.015) \text{ ps}]$ ,<sup>7</sup> we deduce a  $B(M1)$  value for this  $l$ -forbidden transition of  $(53 \pm 9) \times 10^{-3} \mu_N^2$ . In extracting the  $B(M1)$  value we corrected for a 0.47%  $E2$  admixture [ $B(E2) = (33 \pm 2) e^2 \text{fm}^4$ ], which we calculated using the intermediate coupling model of Häuser *et al.*<sup>19</sup> Using FFST, Speth *et al.*<sup>20</sup> calculate  $B(M1) = 20.7 \times 10^{-3} \mu_N^2$  for this transition, while Arima and Huang-Lin<sup>21</sup> get  $B(M1) = 0.03 \times 10^{-3} \mu_N^2$  by taking into account core polarization and pion exchange using Kuo's  $G$  matrix elements. Both calculations account well for the observed quenching (by about a factor of 4 relative to the Schmidt values) of  $l$ -allowed  $M1$  transition rates in the lead region, but systematically underestimate the  $l$ -forbidden  $M1$  rates. Our result reinforces that trend.

To summarize, we have measured the decay rate of the  $l$ -forbidden beta transition  $^{207}\text{Tl}(\frac{1}{2}^+) \rightarrow ^{207}\text{Pb}(\frac{5}{2}^-)$ . We find  $t_{1/2} > 3.6 \times 10^8$  s. This limit is over 2 orders of magnitude greater than the previously established limit. It is useful in distinguishing between model wavefunctions for nuclei around the  $^{208}\text{Pb}$  double-shell closure and ultimately should provide a constraint on the strength of nucleon-meson couplings in heavy nuclei.

## ACKNOWLEDGMENTS

We are grateful to R. U. Khafizov for allowing us to quote his unpublished calculations. This work was supported in part by the U.S. Department of Energy under Contract DE-AC06-81ER40048.

\*Present address: Physics Department, Tennessee Technological University, Cookeville, TN 38505.

†Present address: Kellogg Radiation Laboratory, Caltech 106-38, Pasadena, CA 91125.

‡Present address: National Superconducting Cyclotron Laboratory, Michigan State University, East Lansing, MI 48824.

<sup>1</sup>A. Bohr and B. R. Mottelson, *Nuclear Structure* (Benjamin, New York, 1969), Vol. 1, p. 353.

<sup>2</sup>See, for example, in *Mesons in Nuclei*, edited by M. Rho and D. H. Wilkinson (North-Holland, Amsterdam, 1979), and references therein.

<sup>3</sup>R. Neugart, H. H. Stroke, S. A. Ahmad, H. T. Duong, H. L. Ravn, and K. Wendt, *Phys. Rev. Lett.* **55**, 1559 (1985).

<sup>4</sup>E. G. Adelberger, J. L. Osborne, H. E. Swanson, and B. A. Brown, *Nucl. Phys.* **A417**, 269 (1983).

<sup>5</sup>W. F. Davidson, C. R. Cothorn, and R. D. Conner, *Can. J. Phys.* **45**, 2295 (1967).

<sup>6</sup>F. Nelson, T. Murase, and K. A. Kraus, *J. Chromatog.* **13**, 503 (1964).

<sup>7</sup>*Table of Isotopes*, 7th ed., edited by C. M. Lederer and V. S. Shirley (Wiley, New York, 1978).

<sup>8</sup>C. Briancon, C. F. Leang, and R. Walen, *C. R. Acad. Sci., Ser. B* **266**, 1533 (1968).

<sup>9</sup>L. J. Jardine, *Phys. Rev. C* **11**, 1385 (1975).

<sup>10</sup>*Nucl. Data Sheets* **25**, 397 (1978).

<sup>11</sup>A. Green, quoted by R. O. Mead and J. E. Draper, *Phys. Rev.* **139**, B9 (1965).

<sup>12</sup>S. Gorodetzky, F. A. Beck, T. Byrski, and A. Knipper, *Nucl. Phys.* **A117**, 208 (1968).

<sup>13</sup>Because of the high efficiency and large solid angle that the shield subtends, the dependence of  $P_{\text{sum}} + P_{\text{shield}}$  on angular correlations is expected to be negligible. The value of  $P_{\text{sum}} + P_{\text{shield}}$  for radiation coincident with the 570-keV  $\gamma$  ray is 89.5%. This value is already close to the maximum of 93%, which is the fraction of coincident radiation that escapes the source holder.

<sup>14</sup>F. Rosel, H. M. Fries, K. Adler, and H. C. Pauli, *At. Data Nucl. Data Tables* **21**, 91 (1978).

<sup>15</sup>E. L. Church and J. Weneser, *Ann. Rev. Nucl. Sci.* **10**, 193 (1960).

<sup>16</sup>R. U. Khafizov, private communication.

<sup>17</sup>R. U. Khafizov and S. V. Tolokonnikov, *Phys. Lett.* **153B**, 353 (1985).

<sup>18</sup>R. U. Khafizov, *Phys. Lett.* **162B**, 21 (1985).

<sup>19</sup>O. Häuser, F. C. Khanna, and D. Ward, *Nucl. Phys.* **A194**, 113 (1972).

<sup>20</sup>J. Speth, E. Werner, and W. Wild, *Phys. Rep.* **33**, 127 (1977).

<sup>21</sup>A. Arima and L. J. Huang-Lin, *Phys. Lett.* **41B**, 429 (1972).